

The impact of seasonal variability in wildlife populations on the predicted spread of foot and mouth disease

Author:

Highfield, Linda D; Ward, Michael P; Laffan, Shawn; Norby, Bo; Wagner, Gale G

Publication details:

Veterinary Research

v. 40:18

0928-4249 (ISSN)

Publication Date:

2009

Publisher DOI:

<http://dx.doi.org/10.1051/vetres:2009001>

License:

<https://creativecommons.org/licenses/by-nc-nd/3.0/au/>

Link to license to see what you are allowed to do with this resource.

Downloaded from <http://hdl.handle.net/1959.4/39402> in <https://unsworks.unsw.edu.au> on 2024-04-20

The impact of seasonal variability in wildlife populations on the predicted spread of
foot and mouth disease

L.D. Highfield¹, M.P Ward^{1, 2*}, S.W Laffan³, B.Norby¹, G.G.Wagner⁴

¹ Department of Veterinary Integrative Biosciences, Texas A&M University College
of Veterinary Medicine & Biomedical Sciences, College Station, TX 77845-4458,
USA

² Current address: Faculty of Veterinary Science, The University of Sydney, Private
Mail Bag 3, Camden NSW 2570, Australia

³ School of Biological, Earth and Environmental Sciences, University of New South
Wales, Sydney, NSW 2052, Australia

⁴ Department of Veterinary Pathobiology, Texas A&M University College of
Veterinary Medicine & Biomedical Sciences, College Station, TX 77845-4458, USA

* Corresponding author: m.ward@usyd.edu.au

Running title: Seasonal FMD spread in wildlife populations

Full citation:

Highfield, L.D., Ward, M.P., Laffan, S.W., Norby, B.N. and Wagner, G.G. (2009)
The impact of seasonal variability in wildlife populations on the predicted spread of
foot and mouth disease. *Veterinary Research*, 40:18. DOI:10.1051/vetres:2009001

1 **Abstract**

2 Modeling potential disease spread in wildlife populations is important for predicting,
3 responding to and recovering from a foreign animal disease incursion such as foot and
4 mouth disease (FMD). We conducted a series of simulation experiments to determine
5 how seasonal estimates of the spatial distribution of white-tailed deer impact the
6 predicted magnitude and distribution of potential FMD outbreaks. Outbreaks were
7 simulated in a study area comprising 2 distinct ecoregions in south Texas, USA, using a
8 susceptible-latent-infectious-resistant geographic automata model (Sirca). Seasonal deer
9 distributions were estimated by spatial autoregressive lag models and the normalized
10 difference vegetative index. Significant ($P < 0.0001$) differences in both the median
11 predicted number of deer infected and number of herds infected were found both
12 between seasons and between ecoregions. Larger outbreaks occurred in winter within
13 the higher deer-density ecoregion, whereas larger outbreaks occurred in summer and fall
14 within the lower deer-density ecoregion. Results of this simulation study suggest that
15 the outcome of an FMD incursion in a population of wildlife would depend on the
16 density of the population infected and when during the year the incursion occurs. It is
17 likely that such effects would be seen for FMD incursions in other regions and
18 countries, and for other diseases, in cases in which a potential wildlife reservoir exists.
19 Study findings indicate that the design of a mitigation strategy needs to take into
20 account population and seasonal characteristics.

21

22 spatial modeling / epidemic modeling / foot and mouth disease / wildlife

23 **1. Introduction**

24 Foot and mouth disease (FMD) is a highly contagious, transboundary disease of cloven-
25 hoof animals and one of the most dangerous foreign animal diseases that might be
26 accidentally brought into the USA [8]. Its threat to domestic livestock has been well
27 studied. However, the potential role of wildlife species, which may serve as disease
28 reservoirs, has been largely overlooked. The presence of non-domesticated reservoir
29 species has been a serious obstacle to effective control of FMD outbreaks in other
30 countries [30, 34]. In a series of outbreaks in Britain in 1946, FMD infected deer and
31 European hedgehogs were found near infected livestock premises [30]. In the former
32 Soviet Union, FMD has on numerous occasions been reported to have spread from
33 cattle to Saiga antelope and vice versa. The antelope were reported to have transferred
34 the disease to other species in places far from the original outbreak [30].
35 Deer are among the most commonly FMD-infected wildlife species under field
36 conditions, and are believed to play an important role in the epizootology of FMD [30].
37 The USA has maintained FMD free status since 1929. A 1924 California outbreak
38 involved deer which were exposed via contact from infected cattle¹ [17]. It required 2
39 years to stamp out FMD from the deer population, and over 22 000 were slaughtered in
40 the process¹ [17]. Approximately 10% of those deer slaughtered during the outbreak
41 displayed signs of FMD infection¹.
42 FMD infection in wildlife has also been a concern in more recent FMD outbreaks.
43 During the 2001 FMD outbreak in the U.K. and the Netherlands, it was feared that deer
44 might become infected and potentially act as a reservoir [5, 10, 34]. Evidence of FMD
45 in wild deer was not observed in either of these outbreaks, although there were reports

¹ McVicar J.W., Suttmoller P., Ferris D.H., Campbell C.H., Foot and mouth disease in white-tailed deer: clinical signs and transmission in the laboratory, Proceedings of the 78th Annual Mtg. US Animal Health Association, 1974, pp. 169–180.

46 of wildlife displaying signs of infection [10]. Extensive serosurveillance was conducted
47 after the outbreak, but deer were not tested [10]. Due to the nature of the cattle industry
48 in Europe, a lack of contact between deer and livestock in these countries may have
49 averted a disastrous situation from occurring [10].

50 Since FMD has not been present in the USA for such a lengthy period of time, the entire
51 population of cloven-hoofed animals is susceptible to infection. This includes both
52 livestock and wildlife species. Epidemic models represent an important tool to aid
53 decision making and epidemic response to foreign animal disease incursions such as
54 FMD. Following detection of an incursion of FMD virus in a country previously free of
55 disease, the application of appropriate control measures is a decision that needs to be
56 made rapidly yet with little data. In addition, political, economic and property rights
57 issues may also guide policy decisions regardless of what is deemed to be the most
58 effective strategy to reduce the spread of FMD. Information from model outputs that
59 provide guidance to the probable extent of an outbreak and its time span are invaluable
60 for decision-makers implementing disease control measures in the face of external
61 pressures. Nonetheless, such models need to be developed, validated and tested prior to
62 emergency situations. Strong links between disease modelers, policy and decision-
63 makers also need to exist a priori. Models can serve not only as response and decision-
64 making tools but also as avenues to increase awareness and collaboration with
65 stakeholders.

66 In this research, a simulation model was used to investigate seasonal population impacts
67 on the spread of FMD in wildlife. The development of this model has been previously
68 described [7]. Briefly, it uses a state-transition (susceptible-latent-infectious-resistant,
69 SLIR) framework to simulate the spatial spread of disease within an artificial life model
70 (geographic automata, a generalization of cellular automata). Artificial life models can

71 explicitly incorporate spatial relationships by allowing the interaction between units (for
72 example, individuals or herds) within a population and a predefined neighborhood,
73 based on a set of rules and disease states at earlier time steps. The repetitive application
74 of transmission rules within this local neighborhood replicates the complex spatial
75 behavior that occurs during disease outbreaks. In the Sirca model, the interaction
76 between susceptible herds and infected herds gives rise to newly infected herds. The
77 probability of infection is a function of the distance between herds and the relative size
78 (or density, if a herd occupies a constant land area) of each herd. Thus, spatial
79 arrangements and population density are incorporated into simulated disease spread.
80 The Sirca model has been used to investigate the potential spread of FMD in feral pig
81 populations in Queensland, Australia [7] and in feral pig and wild deer populations in
82 Texas, USA [13, 36].

83 The need to use spatially-explicit simulation models for FMD has been documented [12,
84 16] and spatial heterogeneity has been identified as perhaps the greatest challenge to
85 representing FMD spread across the landscape [8]. Wildlife species are particularly
86 affected by variations in climate and natural resources [13, 36]. To capture spatial
87 heterogeneity across the landscape, wildlife distributions should therefore be seasonally-
88 dynamic [13, 36]. Such temporal dependency may play an important role in the spread
89 of disease within wildlife populations, and further, into domesticated animal populations
90 [7].

91 The study area chosen to investigate how seasonal-dependent variability in wildlife
92 populations might affect the potential spread of FMD is located in south Texas (Fig. 1),
93 and the target species was white-tailed deer (*Odocoileus virginianus*). Texas is the
94 largest cattle production state in the USA and offers the unique opportunity to develop,
95 validate and model the potential impact of foreign animal diseases, such as FMD, in the

96 USA agricultural industry. In general, models developed in Texas to predict areas at-
97 risk of FMD from wildlife reservoirs should be applicable to other ecologically similar
98 areas both in the USA and abroad where potential wildlife reservoirs are present.

99 White-tailed deer represent an important financial resource to a substantial number of
100 ranchers in south Texas [4], and the deer population is actively managed for hunting and
101 recreational purposes [4, 35]. Population management for optimum carrying capacity is
102 important for maintaining nutritional status and population size [37]. Deer in the study
103 area are primarily browsers (consuming leaves and twigs from shrubs and trees) during
104 the autumn [31]. Grasses and forbs have been found to be important dietary components
105 during the spring [11, 19, 26]. Deer will only consume grass when it is tender and green
106 (young), as deer cannot digest mature grass [31]. Forb production in the study area is
107 highly dependent on season (and particularly rainfall); forbs tend to be unpalatable to
108 deer during late summer and late winter [31]. Given this shift in dietary availability,
109 deer distributions are expected to vary by season, specifically based on rainfall and
110 forage availability.

111 The aim of this research was to develop seasonal spatial distributions of wildlife (using
112 the normalized difference vegetation index - NDVI - as a measure of forage availability)
113 and to evaluate how seasonal variability might affect the potential spread of FMD virus.

114 Knowledge of seasonal distributions of wildlife and the impact on the predicted spread
115 of transboundary diseases, such as FMD, can be used to design more effective disease
116 response and mitigation strategies. The specific objectives of this study were to: (1)
117 incorporate seasonal variability into the predicted distribution of white-tailed deer in the
118 study area by using bi-weekly composite NDVI values as a measure of forage
119 availability in a regression model and (2) describe and compare the predicted FMD
120 outbreak distribution that might be observed, given the seasonal variation in the white-

121 tailed deer population distribution.

122

123 **2. Materials and Methods**

124 2.1. *Study site*

125 The study area selected consists of 9 counties located in south Texas, bordering Mexico
126 (Fig. 1). This area contains an estimated population of approximately 427 000 white-
127 tailed deer and consists of two ecoregions – the Edwards Plateau (EP) in the north and
128 the South Texas Brush (ST) in the south – which divide the study region approximately
129 in half (Fig. 1). Seasonal climatic variation in the study area is characterized by hot, dry
130 summers and mild, moist winters, with average annual rainfall ranging between 750 and
131 1200 mm. Drought is common and periodically affects habitat resources and the
132 wildlife population. The Edwards Plateau ecoregion contains the largest white-tailed
133 deer population (estimated one deer per 4 hectares) in Texas². The South Texas brush
134 ecoregion is actively managed to support hunting for white-tailed deer and the
135 population density of deer (estimated one deer per 14 hectares) is considered moderate².

136

137 2.2. *Data source*

138 Bi-weekly composite NDVI images (1 km resolution) for 2006 (n = 26) were obtained
139 for the study area from the United States Geological Survey (USGS) National Mapping
140 Division's Earth Resources Observation and Science (EROS) Data Center. The NDVI is
141 one of a number of vegetative indices derived from remotely sensed imagery. It is
142 associated with photosynthetically active radiation, and is the index most commonly
143 used to estimate vegetative growth [21]. NDVI data are collected by the National
144 Oceanic and Atmospheric Administration's (NOAA) Advanced Very High Resolution

² Texas Parks and Wildlife Department, Wildlife District Descriptions [on line]
http://www.tpwd.state.tx.us/landwater/land/habitats/cross_timbers/ [consulted 22 January 2008].

145 Radiometer (AVHRR) satellite. The index is calculated from measured brightness
146 values based on the absorption, transmittance and reflectance of energy by vegetation in
147 the red and near-infrared portions of the electromagnetic spectrum [6, 15, 24]. To
148 reduce cloud contamination, bi-weekly maximum NDVI composites are created using
149 the maximum observed value for each composite period [9]. NDVI images are
150 registered to the Lambert Equal Area Azimuthal map projection to ensure spatial
151 accuracy to within 1 pixel, where each square pixel is 1 km² in area [32].

152 A baseline predicted distribution of white-tailed deer in the study region was derived by
153 Dasymetric mapping [13]. Dasymetric mapping (also known as surface based
154 demographic data representation) redistributes the population from a set of areal units
155 into either a vector or raster map using ancillary data, such as land use or remotely
156 sensed images [28]. The number of deer per county in the study area was obtained [9]
157 and the distribution of deer was estimated using geostatistical methods, as previously
158 described [13]. Briefly, county-level deer populations were disaggregated, based on
159 suitable land use classes (forest, shrub and grassland) and their estimated class-specific
160 deer carrying capacity. The number of deer per county was then proportionally
161 distributed within land use class and the resulting fractional counts of deer at 30 meter
162 resolution were aggregated to a 1 km² integer grid matching the NDVI images. Each
163 pixel of this grid was assumed to represent a group (herd) of deer. Thus, the grid
164 consisted of location information (the center of each pixel, represented by x and y
165 coordinates) and herd size. Since all square pixels were of a constant area (1 km²), deer
166 herd size is also equivalent to deer herd density in this study. The term ‘herd’ is used
167 subsequently to denote a group of deer, of varying number, occupying a land area of 1
168 km².

169

170 2.3. *Seasonal deer distributions*

171 A seasonal average NDVI coverage was derived and used to represent each of four
172 seasons (winter, spring, summer and autumn) for white-tailed deer distributions. The 26
173 bi-weekly composite NDVI images were converted to raster data sets and projected
174 using the study area polygon coverage (ArcGIS 9.1. ESRI Inc., Redlands, CA, USA).
175 These 26 data sets were subsequently categorized into four seasons (December to
176 February: winter, March to May: spring, June to August: summer, and September to
177 November: autumn). An average NDVI value at the pixel level for each of the seasons
178 was calculated and pixels located within areas of suitable land use classes (forest, shrub
179 and grassland) were extracted (ArcGIS 9.1. ESRI Inc.) by overlaying seasonal average
180 NDVI coverages and the 1992 National Land Cover Dataset³ land use coverage.
181 Regression models were used to describe the seasonal shift in the distribution of deer.
182 The seasonal NDVI was used as an independent variable to predict the number of deer
183 per herd (represented by pixels) as the dependent variable. These data were evaluated
184 for a linear relationship using a correlation coefficient (Stata 10. Stata Corporation,
185 College Station, TX, USA). Ordinary least squares (OLS) regression models were then
186 fit [1] to the data for each season. The residuals of each of these seasonal models were
187 evaluated for the presence of significant ($P < 0.05$) spatial autocorrelation, using a
188 global Moran's I statistic [1]. Significant spatial autocorrelation violates the assumption
189 of independent observations and can bias standard errors, increasing the likelihood of
190 Type I errors. In the case of significant autocorrelation of OLS model residuals,
191 additional spatial diagnostic tests (Lagrange multipliers, LM) were used to determine
192 whether a spatial autoregressive lag or error model should be fit. In cases where the LM

³ U.S. Department of the Interior, U.S. Geological Survey. National Land Cover Dataset 1992 [on line] <http://landcover.usgs.gov> [consulted November 2006].

193 tests for both the spatial lag and spatial error models were significant ($P < 0.05$), both
194 types of models were evaluated and the model with the lowest log likelihood and
195 highest pseudo R^2 statistics was selected. The selection of a lag distance for spatial
196 autoregressive models can often be subjective. For this study, an assumed home range
197 (2 km) for deer [3] was used to generate the weights matrix for the autoregressive lag
198 models. Within a spatial autoregressive model, the coefficient of the spatial lag term (ρ)
199 shows the spatial dependence inherent in the data by measuring the average influence
200 on each observation by their neighboring observations. The selected spatial
201 autoregressive models for each season were evaluated for goodness of fit using a
202 pseudo- R^2 statistic prior to simulating FMD spread within the Sirca model. The
203 residuals of the spatial autoregressive models were also graphically evaluated for
204 normality. The seasonal-specific spatial distributions of predicted number of deer per
205 herd (pixel) were subsequently used as the input data sets within the Sirca simulation
206 model.

207

208 2.4. *Simulation model*

209 The potential spread of FMD, by season and within ecoregion, was simulated using the
210 Sirca model [7, 13, 36]. A conceptualization of disease transmission using the Sirca
211 model is shown in **Figure 2**. In this model, deer herds (represented in this research as
212 pixels) can pass through four disease states: susceptible, latent, infectious and immune.
213 In this study, herd interactions evaluated were restricted to within a 2 km neighborhood
214 distance and to within 8 neighboring herds [13, 36]. When calculating transmission
215 probabilities, herds with more deer than a pre-specified maximum threshold value (30
216 deer per herd in this study) were assigned a probability of 1.0. The densities of the
217 remaining herds were linearly scaled within the interval 0 to 1 by dividing each herd's

size by the maximum threshold value [13, 36]. The probability of FMD virus transmission from one herd to another was calculated as the product of the scaled deer densities of each pair of herds (susceptible and infected) evaluated, modified by the distance (2 km) by which the herds are separated.

To incorporate chance into the model, an interaction between an infected herd and a susceptible neighboring herd (both represented as pixels) resulted in disease transmission when a value from a pseudo-random number generator was below their joint probability threshold [13, 36]. Once a herd was infected the second, third, and fourth transitions in the model depended on the specified length of the latent, infectious and immune periods. Estimates used for these parameters (3 to 5, 3 to 14, and 90 to 180 days, respectively) were derived from previous studies [13, 36]. The specific values for each herd were assigned randomly within the corresponding parameter ranges from a uniform distribution. As in previous studies, homogenous mixing was assumed to take place within (but not between) herds, and the herd was the unit of analysis [13, 36].

The same baseline modeling scenario was used for all model comparisons: to initiate the simulations within each of the 4 seasons, 5 herds (represented as pixels) in each of the 2 ecoregions were randomly selected (SPSS 14.0, SPSS Inc., Chicago, IL, USA) and their status designated as infected. As in previous studies, we randomly selected 5 index herd locations to allow us to simulate the spread of an "average sized outbreak" [36] which included a range of deer-density (low, medium and high) areas and ecoregions. This allowed us to assess the average effect of seasonal variation on predicted FMD spread, without the need to consider the impact of individual site selection issues. For every simulation of the Sirca model, each herd was allowed to interact with other herds within a 2 kilometer neighborhood, representing the home range of deer within the study area.

The model was simulated for a time period representing 90 days (to avoid overlap

243 between seasons) and 100 model runs were simulated for each dataset, yielding a total
244 of 800 model runs ($4 \times 2 \times 100$) and 72 000 model iterations (800×90).

245

246 2.5 Data analysis

247 The seasonal predicted deer distributions (represented by pixels) were described and
248 compared by calculating the minimum, maximum, range, standard deviation, skewness,
249 and kurtosis of the herd size frequency distributions (SPSS, Chicago, IL). From the
250 Sirca model output, the median number of deer infected and the median number of
251 herds (pixels; equivalently, sq. km) were used to characterize each set of simulations
252 ($n = 100$) at the 90th model day for each season ($n = 4$) and ecoregion ($n = 2$). These 8
253 distributions were evaluated for normality (SAS, Cary Institute, NC, USA). A non-
254 parametric Kruskal-Wallis one-way analysis test was used to compare the differences in
255 predicted epidemic spread (measured both by number of deer infected and number of
256 herds infected) between the 8 treatment groups (ecoregion and season). Because the
257 Kruskal-Wallis test only measures significant differences between the highest and
258 lowest groups, a post hoc Miller's multiple comparison test (SAS) was used to evaluate
259 differences between groups.

260

261 3. Results

262 Descriptive statistics for each seasonal deer distribution are shown in Table I. Although
263 the baseline and seasonal-specific mean number of deer (13.96) predicted per herd
264 (pixel) in the study area was constant, compared to the baseline (non-seasonal) deer
265 distribution, seasonal distributions were less variable (as measured by each seasonal-
266 specific distribution's standard deviation and range) but tended to be more positively
267 skewed and kurtotic. Significant ($P < 0.001$) linear relationships between the NDVI and

268 herd size pixels were observed for winter, spring, summer and autumn (respective
 269 correlation coefficients 0.67, 0.60, 0.55 and 0.59). Residuals of each of the four seasonal
 270 ordinary linear regression models showed significant ($P < 0.001$) positive spatial
 271 autocorrelation (Moran's I 0.66, 0.71, 0.72 and 0.72, respectively). In all cases, a spatial
 272 autoregressive lag model was preferred over a spatial autoregressive error model, based
 273 on log likelihood statistics. The characteristics of these fitted seasonal-specific spatial
 274 autoregressive lag models are summarized in Table II. The spatial lag (ρ) terms were
 275 > 0.9 for all seasonal models, indicating that herd size was strongly influenced by
 276 neighboring herd sizes. Residuals of all seasonal spatial autoregressive lag models
 277 visually appeared normally distributed. The spatial distributions predicted using the
 278 autoregressive lag models for each season are shown in Figure 3. Areas of high density
 279 deer distribution were predicted in the north-eastern parts of the study area in all
 280 seasons, and were most extensive in the autumn and winter seasons.

281 The predicted spread of FMD for each season and ecoregion is summarized in Table III
 282 (number of deer) and Table IV (number of herds), and boxplots of the predicted spread
 283 of FMD for each season and ecoregion are shown in Figure 4. There were significant
 284 differences in epidemic spread by both season and ecoregion (Kruskal-Wallis $\chi^2 =$
 285 726.139, $df = 7$, $p\text{-value} < 0.0001$). In all cases a significantly higher median number of
 286 infected deer and infected herds were predicted in the Edwards Plateau ecoregion
 287 (87 792–101 385 deer and 6050–6416 herds) than in the South Texas brush ecoregion
 288 (40 211–54 385 deer and 4336–4969 herds). Miller's multiple comparison test indicated
 289 that within the Edwards Plateau ecoregion, the highest median number of infected deer
 290 (101 385) occurred in winter, with the lowest median number in summer (87 792). The
 291 highest median number of infected herds (6 416) occurred in winter, with the lowest
 292 median number (tied by Miller's test) in spring (6 050) and summer (6 058). Within the

293 South Texas brush ecoregion, the highest (tied by Miller's test) median number of
294 infected deer and herds occurred in autumn (53 389 and 4 969, respectively) and
295 summer (54 385 and 4 922, respectively), with the lowest median number of deer and
296 herds in winter (40 211 and 4 336, respectively). The distributions of predicted infection
297 for outbreaks initiated in winter in the Edwards Plateau and the South Texas brush
298 ecoregions are shown in Figure 5.

299

300 **4. Discussion**

301 Substantial differences were observed in the median predicted magnitude of FMD
302 spread, both by season and ecoregion: the number of deer and herds predicted to be
303 infected ranged from 40 211 deer and 4 336 herds in the South Texas brush ecoregion in
304 winter to 101 385 deer and 6 416 herds in the Edwards Plateau ecoregion in winter.
305 These differences can be explained by changes in modeled deer distribution within the
306 study area, since all other parameters were held constant within this simulation study.
307 Results suggest that the outcome of a transboundary disease incursion (such as FMD) in
308 a wildlife population (such as white-tailed deer in south Texas) might depend on both
309 where and during which time of year the incursion occurs.
310 Spatial autoregressive lag models using the NDVI to predict seasonal-specific deer
311 distributions fit the data well (pseudo $R^2 > 0.8$ for all seasons). Although there were not
312 substantial differences in the overall estimated number of deer in the study area based
313 on the distributions predicted by the spatial autoregressive lag model, the predicted
314 spatial arrangement of the population varied substantially by season (Table I and Figure
315 4), as measured by skewness and kurtosis statistics. Thus, the difference in predicted
316 FMD spread within these populations can be attributed to the spatial distribution
317 patterns of the population – not to differences in the overall size of the population.

318 A significantly ($P < 0.05$) higher number of predicted FMD infected deer and herds
319 were observed in the Edwards Plateau (northern) versus South Texas brush (southern)
320 ecoregion, regardless of season. Within ecoregion, significant ($P < 0.05$) differences in
321 the seasonal number of predicted FMD infected deer and herds was also observed. In
322 the Edwards Plateau ecoregion both the highest number of infected deer and herds were
323 predicted in winter, whereas in the South Texas brush ecoregion the highest numbers
324 were predicted in summer and autumn. These results further support previous work [13]
325 which suggested that the spatial continuity of a population might play an important role
326 in the predicted outbreak size. This result is not surprising, since the Sirca model is a
327 local neighborhood based spatial disease spread model [13]. The more continuity in the
328 spatial distribution, the greater is the opportunity for interactions to occur between
329 herds, consistent with epidemic theory and the importance of spatial heterogeneity [16,
330 18].

331 The model used in this study has been used previously to investigate wildlife-domestic
332 species interactions (feral pigs and cattle [7, 36] and wild deer and cattle [36]) and to
333 evaluate the impact of spatial estimation methodologies on model predicted spread of
334 FMD in deer [13]. In the current study, our focus was on extending previous work to
335 incorporate seasonal variability in white-tailed deer populations and subsequently to
336 predict how the spread of FMD might vary by season. As in previous studies, we
337 modeled only local spread [7, 13, 36]. Given that this is an actively managed and hunted
338 population, there are likely times of the year (hunting season) where potential longer-
339 distance FMD spread may be present.

340 This study focused on the initial stages of disease spread (≤ 90 days) so that the effect of
341 between-season variability in population distributions could be assessed [13]. We also
342 assumed that the home range of deer (2 km) was adequate for creating spatial weights

343 for the spatial autoregressive lag models. Given that deer show high fidelity to their
344 home range, this assumption is likely to be valid [20]. However, the spatial scale of
345 influence of the surrounding population on seasonal deer distribution is unknown.
346 Future work should incorporate a range of spatial weights and assess how this variation
347 might impact model predictions of deer distribution.

348 The behavior of wildlife species is also seasonally-variable and should be included in
349 future work focusing on the spread of FMD in wildlife populations. For example, the rut
350 (breeding season) in white-tailed deer in the study area typically occurs in the Edwards
351 Plateau ecoregion between October and December, and in the South Texas brush
352 ecoregion in December⁴. During this time of the year, bucks are more likely to move
353 around and cover larger distances than normal⁴. This could contribute substantially to
354 increased spread of FMD because of greater numbers of interactions with other
355 potentially susceptible deer. Juvenile males will also disperse from their female groups
356 and an increase in the number of single males in the population may need to be modeled
357 [27]. In addition, a stable population (no births or deaths) was assumed in this study
358 because of the relatively short (≤ 90 days) time periods simulated. Future studies should
359 incorporate such changes in the population structure, especially given that this area is
360 intensively managed for hunting and recreation.

361 An assumption was made in this study that the same spatial relationship for predicting
362 deer distributions (in the autoregressive lag models) was valid over the entire study area
363 (both ecoregions). Ecoregions comprise similar soils, topography, land use and
364 vegetation (habitat). Given the substantial differences in the modeled spatial distribution
365 of deer in the two ecoregions in the study area, it is likely that some variation in the

⁴ Texas Parks and Wildlife Department. The rut in white-tailed deer [on line]
http://www.tpwd.state.tx.us/huntwild/hunt/planning/rut_whitetailed_deer/ [consulted 24
January 2008].

366 spatial relationship may exist. Future work should examine the application of regression
367 models specific to ecoregions to determine if substantial variation does exist and
368 whether this might impact predicted disease spread. If there are substantial differences
369 in the spatial distributions of deer by ecoregion there is utility in developing separate
370 ecoregion-specific regression models. However, the usefulness of ecoregion as a
371 predictor for estimating deer distributions might be limited because some of the habitat
372 variability is captured at a finer resolution with land use data. Using ecoregions as a
373 marker for modeling deer behavior might also be limited because regions are a very
374 broad scale measurement of the environment and have no associated attribute data.
375 While it might be useful to model deer behavior with a larger number of finer resolution
376 ecoregions, it becomes exceedingly complex: as data requirements increase, a greater
377 number of variables have to be estimated and information on behavior within a
378 particular ecoregion has to be derived from expert opinion. This greatly adds to
379 uncertainty in the resulting estimates.

380 The NDVI has been used in numerous studies on the classification of land use and
381 temporal vegetation variability (onset, peak, senescence) [23, 32]^{5,6,7}, as well as the
382 examination of the relationship between NDVI and livestock stocking rates in the USA
383 [14, 29]. The NDVI was highly correlated ($R^2 > 0.7$) with dietary measurements of
384 white-tailed deer during winter and spring in north central Texas [33], and the NDVI

⁵ Turcotte K., Dramber W., Venugopal G., Lulla K., Analysis of region-scale vegetation dynamics of Mexico using stratified AVHRR NDVI data, Proceedings of the Annual Society for Photogrammetry and Remote Sensing, Baltimore, MD, USA, 1989.

⁶ Hochheim K., Bullock P., Operational estimates of western Canada spring wheat yield using NOAA/AVHRR LAC data, Proceedings of the 12th Pecora Symposium, Bethesda, MD, USA, 1994.

⁷ vanLeeuwen W., Huete A., Begue A., Duncan J., Franklin J., Hanan N., et al., Evaluation of vegetation indices for retrieval of soil and vegetation parameters at Hapex-Sahel, Proceedings of the 12th Pecora Symposium, Bethesda, MD, USA, 1994.

385 was significantly ($P < 0.05$) associated with mule deer distributions in the southwest
386 desert in spring, summer and autumn [25]. In the present study, a single year of NDVI
387 data was used and bi-weekly measurements were grouped into a seasonal average to
388 predict deer distributions. As documented in previous studies [25, 33], a traditional
389 seasonal (winter, spring, summer, autumn) breakdown was assumed to be appropriate.
390 More detailed analysis of methods of grouping NDVI data for predicting deer
391 distribution is warranted, as the traditional seasonal approach may not adequately
392 capture seasonal variability in the relationship between vegetative greenness and forage
393 availability. It was further assumed that one year of NDVI data was adequate to model
394 seasonal variability. This assumption is valid if the interest in modeling deer distribution
395 focuses on the most recent year; however, longer term trends may also be of interest to
396 modelers and policy decision-makers. Future work on a short time series might provide
397 a better understanding of the broad patterns of NDVI over time in the study area.

398 There are numerous areas of the USA where livestock are extensively grazed and the
399 potential for interaction with susceptible wildlife species, such as white-tailed deer, is
400 high. Deer move through and forage in fields between farms and enter premises with
401 animal feed and slurry [34]. In addition, supplemental feeding of white-tailed deer for
402 hunting purposes is a common practice in many areas of the USA [14]. Deer densities in
403 parts of Texas are very high, and most deer inhabit private land [22]. As the result of
404 extensive land use change, deer populations in Texas have formed metapopulations with
405 high deer densities, increased contact between deer populations and potentially the risk
406 of disease transmission to domestic livestock [22]. Based on a review of the literature,
407 the current study is probably only one of two [7] to incorporate seasonal variability in
408 wildlife distributions and to define the potential magnitude of an FMD outbreak by
409 season. Substantial seasonal variability in the model predicted spread of FMD was

410 found. Future work focusing on improved methods of analysis of NDVI data, spatial
411 regression models and incorporating behavioral traits are needed to yield additional
412 insights into the potential spread of transboundary diseases, such as FMD, in wildlife
413 populations.

414 In this simulation study, the outcome of an FMD incursion was found to depend on both
415 when and where the incursion occurred. These results are important to consider when
416 designing disease mitigation strategies. It is likely that such effects would be seen for
417 FMD incursions in other regions and countries, and for other diseases, in cases in which
418 a potential wildlife reservoir exists.

419

420 **Acknowledgements**

421 This study represents research by the senior author in partial fulfillment for the degree
422 of PhD in Biomedical Sciences, College of Veterinary Medicine & Biomedical
423 Sciences, Texas A&M University. Partial funding for this study was provided to MPW
424 by the Foreign Animal and Zoonotic Disease Defense Center, A Department of
425 Homeland Security National Center of Excellence at Texas A&M University.

426 **References**

- 427 [1] Anselin L., GeoDa 0.9 User's Guide. Spatial Analysis Laboratory, University of
428 Illinois, Urbana-Champaign, IL., 2003.
- 429 [2] Bartoskewitz M.L., Hewitt D.G., Pitts J.S., Bryant F.C., Supplemental Feed Use by
430 Free-Ranging White-Tailed Deer in Southern Texas, Wildlife Soc. Bull. (2003)
431 31:1218–1228.
- 432 [3] Cohen W.E., Drawe D.L., Bryant F.C., Bradley L.C., Observations on white-tailed
433 deer and habitat response to livestock grazing in south Texas, J. Range Management
434 (1989) 42:361–365.
- 435 [4] Cooper S.M., Owens M.K., Cooper R.M., Ginnett T.F., Effect of supplemental
436 feeding on spatial distribution and browse utilization by white-tailed deer in semi-arid
437 rangeland, J. Arid Environ. (2006) 66:716–726.
- 438 [5] Davies G., Foot and mouth disease, Res. Vet. Sci. (2002) 73:195-199
- 439 [6] Derring D., Haas R., Using Landsat Digital Data for Estimating Green Biomass,
440 Technical Memorandum 80727, National Aeronautics and Space Administration, USA,
441 1980.
- 442 [7] Doran R.J., Laffan S.W., Simulating the spatial dynamics of foot and mouth disease
443 outbreaks in feral pigs and livestock in Queensland, Australia, using a susceptible-
444 infected-recovered cellular automata model, Prev. Vet. Med. (2005) 70:133–152.
- 445 [8] Durand B., Mahul O., An extended state-transition model for foot and mouth disease
446 epidemics in France, Prev. Vet. Med. (2000) 47:121–139.
- 447 [9] Eidenshink J.C., Conterminous U.S. AVHRR data set, Photogramm, Eng. Remote
448 Sens. (1991) 58:809–813.
- 449 [10] Elbers A.R.W., Dekker A., Dekkers L.J.M., Serosurveillance of wild deer and wild
450 boar after the epidemic of foot-and-mouth disease in the Netherlands in 2001, Vet. Rec.

451 (2003) 153:678-681.

452 [11] Everitt J.H., Drawe D.L., Spring food habits of white-tailed deer in the south Texas
 453 plains, J. Wildl. Management (1974) 27:15-20.

454 [12] Garner M.G., Lack M., An evaluation of alternate control strategies for foot and
 455 mouth disease in Australia: a regional approach, Prev. Vet. Med. (1995) 23:9-32.

456 [13] Highfield L., Ward M.P., Laffan S.W., Representation of animal distributions in
 457 space: how geostatistical estimates impact simulation modeling of foot-and-mouth
 458 disease spread, Vet. Res. (2008) 39:17.

459 [14] Hunt E.R. Jr., Miyake B.A., Comparison of stocking rates from remote sensing and
 460 geospatial data, Range. Ecol. Management (2006) 59:11-18.

461 [15] Jensen J., Introductory digital image processing prentice-hall, Englewood Cliffs,
 462 NJ, 1996.

463 [16] Kao R.R., The impact of local heterogeneity on alternative control strategies for
 464 foot-and-mouth disease, Proc. Biol. Sci. (2003) 270:2557-2564.

465 [17] Keane C., The epizootic of Foot-and-Mouth Disease in California, Calif. Dept.
 466 Agric. Special Pub. No. 65, 1926, 54 pp.

467 [18] Keeling M.J., The effects of local spatial structure on epidemiological invasions,
 468 Proc. Biol. Sci. (1999) 266:859-869.

469 [19] Kelley J.A., 1970. Food habits of our exotic big game animals on a Texas Hill
 470 Country ranch. MS Thesis, Texas A&M Univ., Kingsville, TX. 101pp.

471 [20] Kilpatrick H.J., Spohr S.M., Lima K.K., Effects of population reduction on home
 472 ranges of female white-tailed deer at high densities, Can. J. Zool. (2001) 79:949-954.

473 [21] Kitron U., Kazmierczak J., Spatial Analysis of the Distribution of Lyme Disease in
 474 Wisconsin, Am. J. Epidemiol. (1997) 145:558-566.

475 [222] Lockwood M., White-tailed deer population trends. Performance report as

476 required by federal aid in wildlife restoration act, project number: W-127-R-13. 31-Jul-
 477 2005. Texas Parks and Wildlife, Austin, TX, 2005.

478 [23] Loveland T.R., Merchant J.W., Ohlen D.O., Brown J.F., Development of a land-
 479 cover characteristics database for the conterminous U.S., Photogramm. Eng. Remote
 480 Sens. (1991) 57:1453–1463.

481 [24] Lyon J.G., McCarthy J., Wetland and Environmental Applications of GIS, Lewis
 482 Publishers, Boca Raton, FL, 1995.

483 [25] Marshall J.P., Bleich V.C., Krausman P.R., Reed M.L., Andrew N.G., Factors
 484 affecting habitat use and distribution of desert mule deer in an arid environment, Wildl.
 485 Soc. Bull. (2006) 34:609–619.

486 [26] McMahan C.A., Comparative food habits of deer and three classes of livestock, J.
 487 Wildl. Manage. (1964) 28:798–808.

488 [27] McCoy E.J., Hewitt D.G., Bryant F.C., Dispersal by yearling male white-tailed deer
 489 and implications for management, J. Wildl. Manage. (2005) 69:366-376.

490 [28] Mennis J., Generating surface models of population using dasymetric mapping,
 491 Prof. Geogr. (2003) 55:31-42.

492 [29] Oesterheld M., DiBella C.M., Kerdiles H., Relation between NOAA-AVHRR
 493 satellite data and stocking rate of rangelands, Ecol. Appl. (1998) 8:207-212.

494 [30] Pinto A.A., Foot-and-mouth disease in tropical wildlife, Ann. NY Acad. Sci.
 495 (2004) 1026:65-72.

496 [31] Rutledge J., Bartoskewitz T., Brown K., Comprehensive Wildlife Management
 497 Planning Guidelines for the South Texas Ecological Region. Texas Parks and Wildlife
 498 Department, Austin, Texas, 2001.

499 [32] Senay G.B., Elliott R.L., Combining AVHRR-NDVI and landuse data to describe
 500 temporal and spatial dynamics of vegetation, Forest Ecol. Management (2000) 128:83-

501 91.

502 [33] Showers S.E., Tolleson D.R., Stuth J.W., Kroll J.C., Koerth B.H., Predicting diet
503 quality of white-tailed deer via NIRS fecal profiling, *Range. Ecol. Management* (2006)
504 59:300-307.

505 [34] Suttmoller P., Barteling S.S., Olascoaga R.C., Sumption K.J., Control and
506 eradication of foot-and-mouth disease, *Virus Res.* (2003) 91:101-144.

507 [35] Thigpen J., Adams C.E., Thomas J.K., Texas Hunting Leases, Leaflet-2441, Texas
508 Agricultural Extension Service, College Station, TX, 1990.

509 [36] Ward M.P., Laffan S.P., Highfield L.D., The potential role of wild and feral
510 animals as reservoirs of foot-and-mouth disease, *Prev. Vet. Med.* (2007) 80:9-23.

511 [37] Warren R.J., Krysl L.J., White-tailed deer food habits and nutritional status as
512 affected by grazing and deer harvest management, *J. Range. Management* (1983)
513 36:104-109.

Figure 1. A study area in south Texas selected to evaluate how seasonal variability in the distribution of white-tailed deer might affect the potential spread of foot and mouth disease. Two ecoregions (the Edwards Plateau (EP) and South Texas Brush) represented in this study area are shown. The location of the 9 counties forming the study area, bordering Mexico, is shown in the insert.

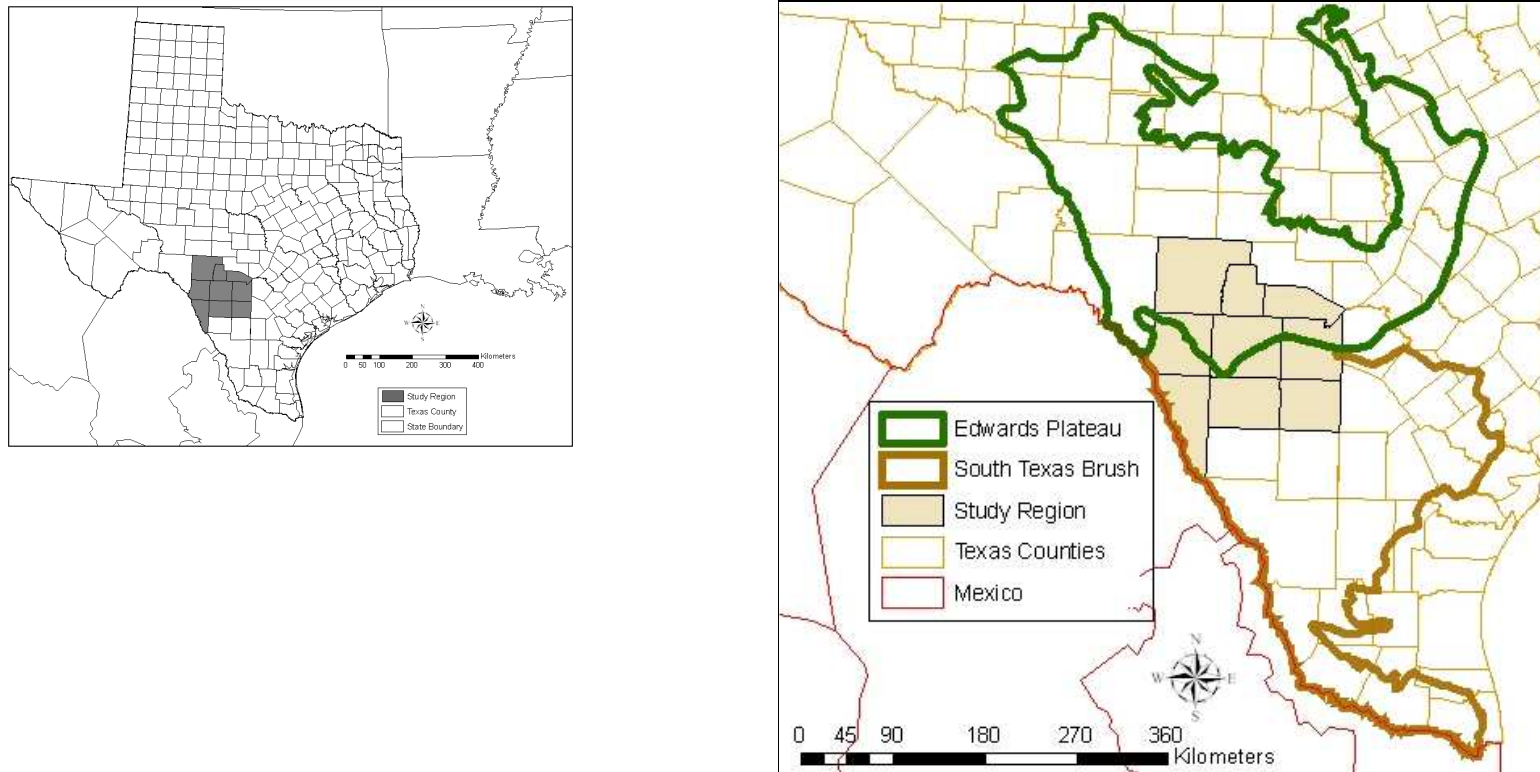


Figure 2. Conceptualization of modeling disease transmission in Sirca (A through D).

A. 8 neighbors evaluated as potential contacts from the source infected cell (center, bold outline). Each cell represents a “herd” of deer with the raw density value shown for each.

6	3	13
9	20	29
1	5	11

B. Scaled density of all herds (infected and susceptible) is calculated using 30 deer per km² as the threshold value. Ex: $20/30 = 0.67$ (source infected cell; center, bold outline).

0.2	0.1	0.43
0.3	0.67	0.97
0.03	0.17	0.37

C. Probability of FMD virus transmission is calculated as the product of the scaled densities for the source infected cell and each of the 8 potential contacts. Cells show probabilities for contact between the center and its 8 neighboring cells. Ex: the probability of transmission to the eastern cell (shown in gray) is $0.67 * 0.97 = 0.65$.

0.134	0.067	0.288
0.201		0.65
0.0201	0.114	0.248

D. Probability of FMD virus transmission is then modified by the spatial kernel to account for distance between potential contacts. In this case the kernel is the cell size (1) divided by the distance between cells. Modified contact probabilities are shown in gray. Ex: the probability of transmission to the north-western cell is $0.67 * 0.134 * \sqrt{2} = 0.095$.

0.095	0.067	0.204
0.201		0.65
0.014	0.114	0.175

An interaction between the source infected cell and a susceptible neighboring cell results in disease transmission when a value drawn from a pseudo-random number generator is below the modified contact probability (shown above) of the evaluated contact.

Figure 3. Seasonal-specific white-tailed deer distributions in a study area in south Texas selected to evaluate the effect of seasonal variability on potential spread of foot and mouth disease. Distributions were predicted using the normalized difference vegetation index and spatial autoregressive lag models (Tab. II).

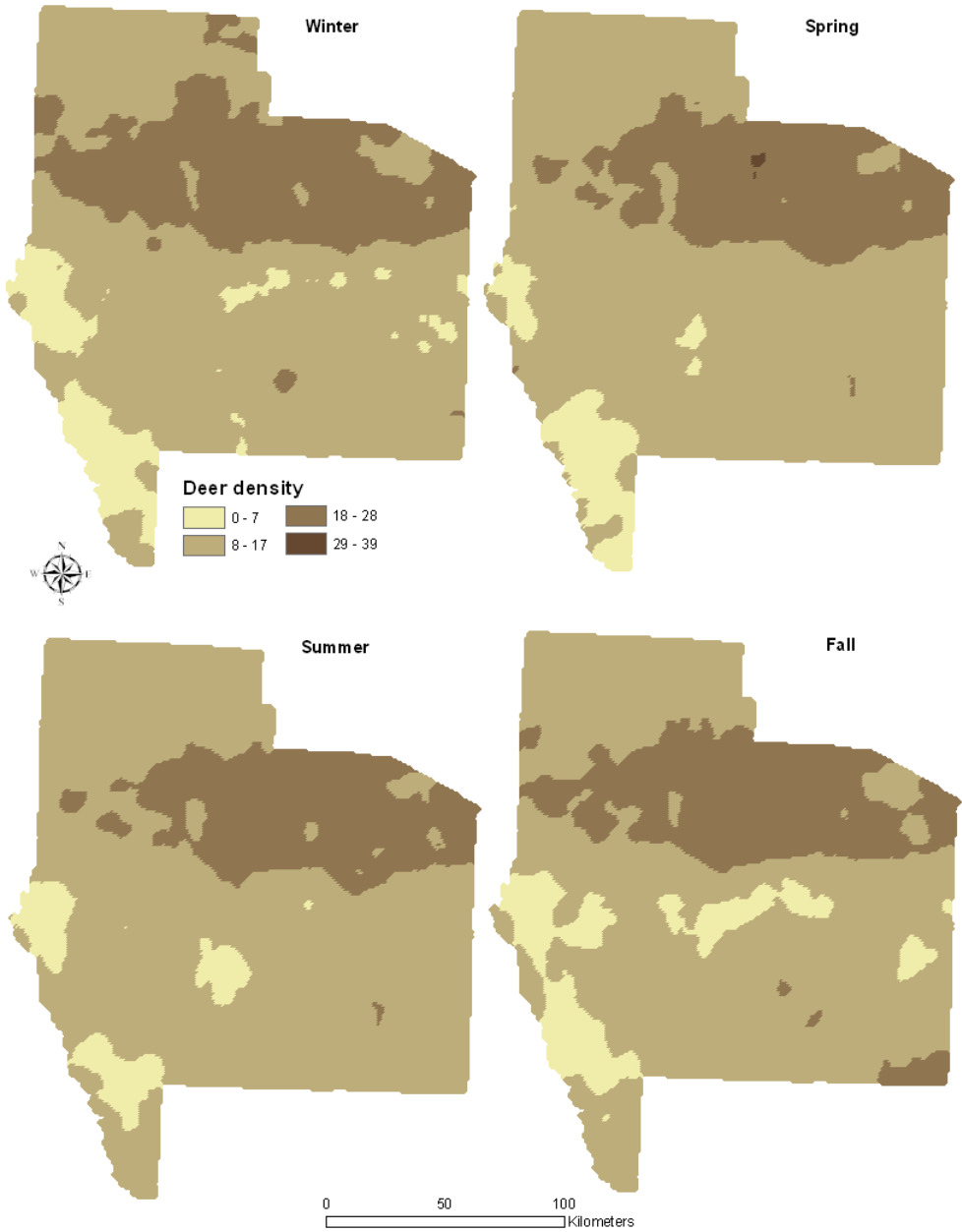


Figure 4. Foot and mouth disease infection of white-tailed deer (upper) and deer herds (lower) in an area in south Texas, predicted by 100 simulations of a susceptible-latent-infectious-resistant geographic automata model (Sirca).

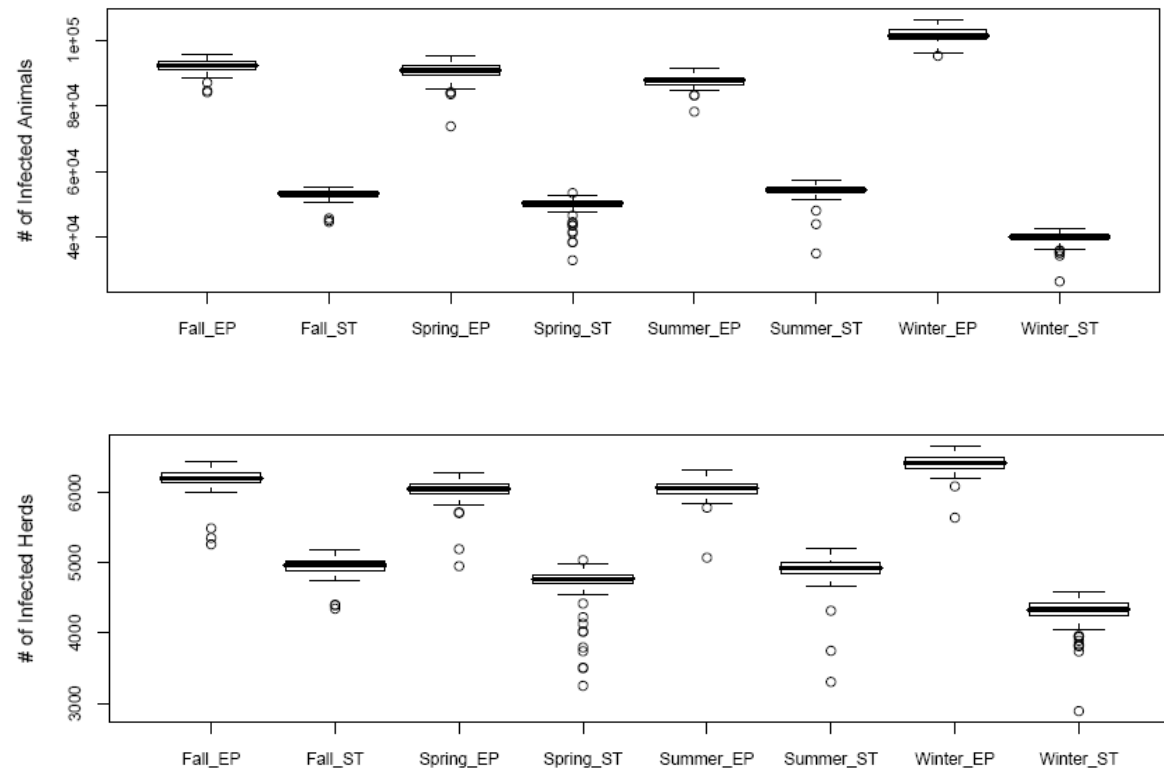


Figure 5. Probability of foot and mouth disease infection of winter-distributed white-tailed deer in an area in south Texas, predicted by 100 simulations of the Sirca model. Each simulation was initiated at the same 5 index herds (●, represented as 1 km² pixels) in either the Edwards Plateau (upper) or South Texas Brush (lower) ecoregions as infected. Probability of infection (per pixel) is shown.

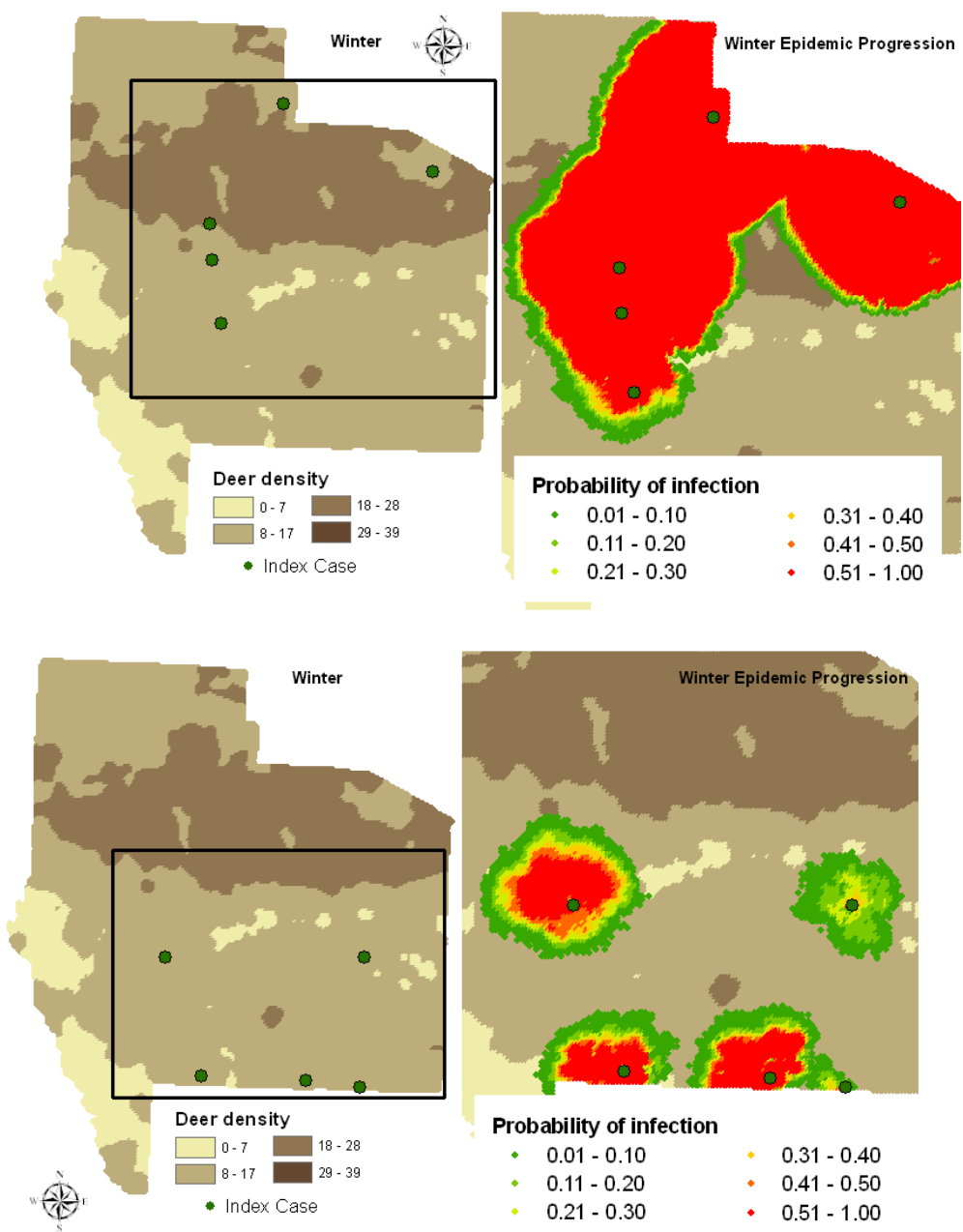


Table I. Descriptive statistics for white-tailed deer distributions (represented by 1

km² pixels) predicted in an area of south Texas, using information from the normalized difference vegetation index and an estimated baseline (non-seasonal) deer distribution (427 292 deer in 30 592 herds, spatially represented as pixels). Seasonal-specific mean number of deer (13.96) predicted per herd (pixel) in the study area was constant.

Distribution	SD	Minimum	Maximum	Range	Skewness	Kurtosis
Baseline	8	0	36	36	0.35	1.94
Winter	6	1	28	27	0.61	2.28
Spring	5	3	29	26	0.75	2.94
Summer	4	5	27	22	0.54	2.92
Autumn	5	0	27	27	0.39	2.67

Table II. Characteristics of spatial autoregressive lag models fitted to seasonal white-tailed deer distributions (represented spatially by 30 592, 1 km² pixels) in an area of south Texas, derived using the normalized difference vegetation index.

Model	Parameters	Constant	NDVI	Spatial lag, ρ
Winter	Coefficient	-1.41	6.06	0.918
	Std. error	0.028	0.096	0.003
	z-value	-14.67	21.08	284.7
	probability	< 0.001	< 0.001	< 0.001
Pseudo R ² = 0.837				
Spring	Coefficient	-1.2	5.2	0.932
	Std. error	0.105	0.305	0.003
	z-value	-11.36	17.04	313.3
	probability	< 0.001	< 0.001	< 0.001
Pseudo R ² = 0.838				
Summer	Coefficient	-0.88	4.17	0.938
	Std. error	-1.02	0.28	0.003
	z-value	-8.64	14.7	331.7
	probability	<0.001	<0.001	<0.001
Pseudo R ² = 0.838				
Autumn	Coefficient	-1.33	4.91	0.932
	Std. error	0.11	0.29	0.003
	z-value	-11.76	17.0	313.6
	probability	< 0.001	< 0.001	< 0.001
Pseudo R ² = 0.838				

Table III. Predicted size (number of deer infected) of an outbreak of foot-and-mouth disease in a population of white-tailed deer in an area of south Texas for each season by ecoregion (Edwards Plateau and South Texas brush). Results shown are from 100 simulations of a susceptible-latent-infectious-resistant geographic automata model (Sirca) for each seasonal deer distribution.

Ecoregion	Season	Deer				
		Median	Interquartile range	25%, 75% percentile	Skewness	Kurtosis
Edwards Plateau	Winter	101385	2868	100305, 103239	-0.19	-0.20
Edwards Plateau	Spring	90913	2885	89233, 92139	-2.28	10.5
Edwards Plateau	Summer	87792	2082	86612, 88707	-1.14	4.6
Edwards Plateau	Autumn	92323	2314	91126, 93445	-.92	2.07
South Texas brush	Winter	40211	1819	39205, 41086	-2.9	13.9
South Texas brush	Spring	50372	1330	49502, 50866	-2.9	10.1
South Texas brush	Summer	54385	1753	53462, 55233	-4.7	29.8
South Texas brush	Autumn	53389	1546	52515, 54074	-3.01	11.7

Table IV. Predicted size (number of deer herds infected) of an outbreak of foot-and-mouth disease in a population of white-tailed deer in an area of south Texas for each season by ecoregion (Edwards Plateau and South Texas brush). Results shown are from 100 simulations of a susceptible-latent-infectious-resistant geographic automata model (Sirca) for each seasonal deer distribution.

Ecoregion	Season	Deer Herds				
		Median	Interquartile range	25%, 75% percentile	Skewness	Kurtosis
Edwards Plateau	Winter	6416	154	6340, 6496	-1.9	9.3
Edwards Plateau	Spring	6050	139	5972, 6112	-3.3	16.3
Edwards Plateau	Summer	6058	131	5983, 6115	-3.4	22.5
Edwards Plateau	Autumn	6198	142	6138, 6281	-3.1	12.9
South Texas brush	Winter	4336	186	4247, 4436	-2.9	13.6
South Texas brush	Spring	4766	117	4696, 4815	-2.8	7.9
South Texas brush	Summer	4922	161	4842, 5004	-4.2	23.6
South Texas brush	Autumn	4969	132	4891, 5023	-2.2	7.5